ELSEVIER

Fabrication of excitonic luminescent inorganic–organic hybrid nano- and microcrystals

I. Saikumar,[a] Shahab Ahmad,[a] J.J. Baumberg[b] and G. Vijaya Prakash[a,*]

[a]Nanophotonics Lab, Department of Physics, Indian Institute of Technology Delhi, New Delhi 110 016, India
[b]Nanophotonics Centre, Cavendish Laboratory, University of Cambridge, Cambridge CB3 0HE, UK

Inorganic–organic (IO) hybrid nano- and microcrystals are fabricated by a low-cost, environmentally friendly and easily scaled-up route. Lead(II) iodide (PbI_2) nano/microcrystals are obtained by solvothermal techniques and subsequent IO hybrid ($(C_{12}H_{25}NH_3)_2PbI_4$) crystals are produced by intercalation of the organic moiety. The hexagonally shaped crystals obtained range in size from 20 nm to $\sim$7 μm. Sequential stacking of inorganic/organic layers in these IO hybrid crystals results in strong room-temperature exciton photoluminescence, wherein the excitons are confined within the inorganic sheets.
© 2012 Acta Materialia Inc. Published by Elsevier Ltd. All rights reserved.

Keywords: Room-temperature excitons; Intercalation compounds; Layered structures; Microstructure; Inorganic–organic framework material

The optical properties of soft materials have attracted attention for a number of years due to their potential applications in optoelectronic devices. An increasing number of studies focus on hybrid inorganic–organic (IO) materials [1], due to the possibility of combining the diverse properties of inorganic (high mobility, electrical pumping, band engineering) and organic (low-cost technology, high luminescence quantum yields, room temperature) performance. In this context, IO hybrids of chemical formula $(R-NH_3)_2MX_4$, where R is an organic moiety, M is a divalent metal (Pb^{2+}, Sn^{2+}, Cu^{2+}, Cd^{2+}, etc.) and X is I^-, Cl^- or Br^-, represent a natural hybrid IO system. These perovskite-type structures possess structural flexibility that can be tailored by substituting different halides [2,3] as well as various organic moieties [4]. Tremendous interest has been shown both for fundamental studies and for applications in optoelectronics and photonics [2–5].

A recent successful approach to fabricate device-compatible IO hybrids is based on inserting appropriately sized organic guest moieties into the empty spaces within a crystalline host. Layered semiconductor compounds (e.g. PbI_2, SnI_2) exhibit anisotropic confinement along different crystallographic axes [6]. Lead iodide (PbI_2) has a structural repeat unit of hexagonally closed-packed I–Pb–I molecular layers which are separated by a gap of 6.78 Å with the layers stacked perpendicularly along the c-axis [7–9]. Compared to conventional synthesis, the intercalation of organic moieties into PbI_2 to obtain the desired IO hybrids ($(R-NH_3)_2PbI_4$) is relatively easy and yields well-ordered centimeter-sized films [10]. The kinetics of inorganic and organic layer formation typically depends on the nature and shape of the guest moiety, the concentration of guest molecules and the solvent used [10]. The organic moiety conformation results in variations in the sequence of stacking layers along the layer normal to the hexagonal c-axis [11]. Due to the presence of alternate layered arrangements of Pb–I and organic networks, these IO hybrids exhibit remarkably strongly bonded excitons ($E_b \sim 200$ meV) which are even observable at room temperature. This is due to the effects of dielectric mismatch and quantum confinement in the semiconductor layers that hold the electronic carriers [12]. As a consequence, these IO hybrids are considered to be "natural" inorganic–organic multiple quantum wells (IO-MQWs) which show strong and narrow absorption and photoluminescence at room temperature.

Conventional synthesis of these IO hybrids includes sol–gel processing methods for thin film formation [10,13,14] and single-crystal harvesting methods [13,15–18]. However, such IO-MQWs are difficult to fabricate directly into nano- and microscale structures.

---

* Corresponding author. Tel.: +91 (11) 2659 1326; fax: +91 (11) 2658 1114; e-mail: prakash@physics.iitd.ac.in

Growth of highly anisotropic inorganic low-dimensional structures, by controlling the size and morphology through a single-step process and at relatively low temperatures, is a formidable task but is highly desirable for many new types of optoelectronic devices.
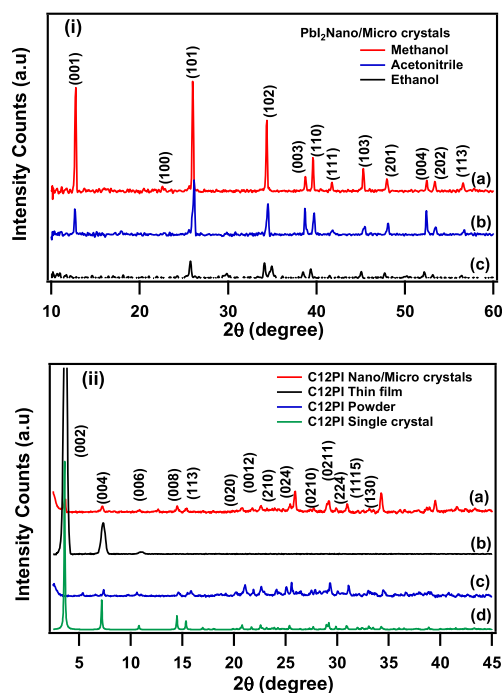
In this paper we demonstrate a novel and simple methodology for the fabrication of highly anisotropic and efficiently luminescent IO hybrids into nano/micro-scale crystals. This method follows a two-step process: first, preparation of PbI_2 nano/microcrystals by a solvo-thermal method [6]; and then their complete conversion into IO hybrids via a newly developed intercalation process using pre-synthesized organic moieties [10]. The structural, morphological and optical properties of these strongly emissive IO hybrid nano/microcrystals show the success of this approach.

PbI_2 nano/microcrystals were synthesized at room temperature using an aqueous solution of potassium iodide (KI) and lead nitrate ($Pb(NO_3)_2$) in methanol, ethanol and acetonitrile solvents [6]. 5 ml of 0.01 M aqueous solution of lead nitrate was added to 100 ml of the solvent of interest. Into this solution, under vigorous ultrasonic homogenization, 5 ml of 0.05 M aqueous KI was added. The sudden appearance of a yellow colour by the addition of KI is the first evidence of the formation of PbI_2 crystallites. The PbI_2 crystals thus formed were collected carefully and dried at 60 °C. The crystal growth and size are critically dependent on concentrations of the constituents, the use of different host solvents, separation time and temperature. While the obtained crystals are of various nano/micron dimensions, nanosized crystals are directly obtained from the supernatant solutions and used for analysis.

To obtain IO hybrid nano/microcrystals of dodecyl-lammonium tetraiodo plumbate, $(C_{12}H_{25}NH_3)_2PbI_4$ (hereafter C12PI), pre-synthesized organic iodide solutions of $C_{12}H_{25}NH_3I$ (hereafter C12I) in toluene (40 mg/5 ml) are used in an intercalation process as explained in an earlier communication [10]. We also demonstrate the approach using another organic iodide $C_6H_9C_2H_4NH_3I$ (hereafter CHI) to obtain IO hybrid crystals of 2(1-cyclohexenyl) ethylammonium tetraiodo plumbate (($C_6H_5C_2H_4NH_3)_2PbI_4$) (hereafter CHPI) for comparison.

The prepared PbI_2 nano/microcrystals were characterized by thin-film/powder X-ray diffraction (XRD) in for the 2θ range from 10° to 60° to determine the phase purity and crystallinity. XRD pattern of nano/microcrystals of PbI_2 prepared in various solvents (methanol, acetonitrile and ethanol) are shown in Figure 1(i). All the peaks in the XRD pattern indicate the pure hexagonal structure (JCPDS Card No. 79-0803) with space group *P-3m1*(164). The strong diffraction peaks of PbI_2 nano/microcrystals in Figure 1(i) indicate high crystallinity and a layered structure with plane separation $d = 6.78$ Å along the *c*-axis.

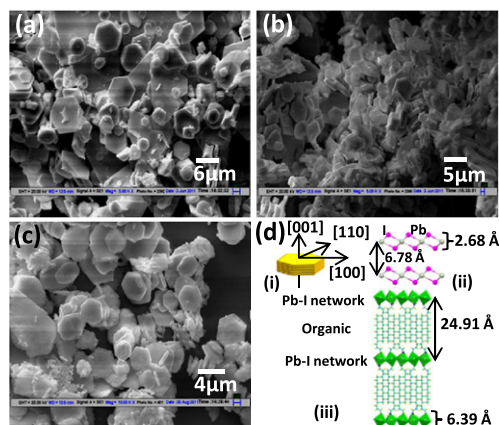The unit cell parameters (*a = b* and *c*) of the prepared PbI_2 nano/microcrystals are found to be 4.544 and 6.937 Å (methanol), 4.507 and 6.974 Å (acetonitrile) and 4.575 and 7.083 Å (ethanol), respectively, which are highly compatible with reported data (*a = b =* 4.557 Å, *c* = 6.979 Å) [19]. Furthermore, relative broadening occurred in the observed XRD peaks for the PbI_2

Figure 1. (i) XRD patterns of PbI_2 nano/microcrystals prepared from (a) methanol, (b) acetonitrile and (c) ethanol. (ii) XRD patterns of C12PI as (a) intercalated nano/microcrystals (PbI_2 prepared in methanol), (b) thin films, (c) powder and (d) simulated C12PI XRD patterns from single-crystal XRD analysis.

crystals (Fig. 1(i)c) synthesized in ethanol compared to methanol and acetonitrile. The peak related to [0 0 1] is also absent in PbI_2 crystals prepared in ethanol, though the reason for this is unclear at present. The PbI_2 crystals thus prepared were used to prepare IO hybrid crystals using this intercalation process [10]. Figure 1(ii)a shows that after intercalation with C12I there is a complete conversion of PbI_2 crystals (Fig. 1(i)a) into the desired C12PI. Due to this intercalation, the spacing between Pb–I layers is substantially increased, as seen from the shift in the diffraction peaks to low angles. The strong [0 0 2] reflection of C12PI crystals corresponds to an interlayer distance of 24.08 Å separating the inorganic sheets [20], which is in accordance with the spacing (24.91 Å) obtained from single-crystal XRD analysis [16]. The comparison is shown (Fig. 1(ii)) between the XRD patterns of conventionally fabricated C12PI thin films, powder and single-crystal XRD data [10]. In the XRD pattern of C12PI powder, the missing [0 0 2] peak indicates the lack of a layered arrangement, whereas [0 0 1] reflections are prominent in thin film, which suggests that the alternating organic/inorganic layers stack perpendicular to the substrate surface.

SEM images reveal the hexagonal shape of the PbI_2 crystals extracted by filtration from methanol (Fig. 2a), acetonitrile (Fig. 2b) and ethanol [21], with average diameter of 5, 4 and 1.5 μm respectively, with meagre variation in average thickness (400 ± 100 nm). The hexagonal shape of these crystals is assumed to be due to the strong interaction between the Pb(II) and I_2 molecules in the solvothermal system [6], which controls the
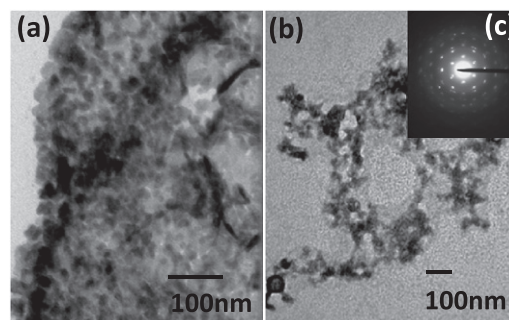
Figure 2. SEM images of the PbI$_2$ nano/microcrystals synthesized via the solvothermal method in (a) methanol and (b) acetonitrile. (c) C12PI nano/microcrystals (PbI$_2$ prepared in acetonitrile) intercalated for 10 s. (d) (i) Schematic diagram of hexagonally shaped lead iodide crystal showing directions of crystal growth [0 0 1] (c-axis), [1 0 0] and [1 1 0] directions; (ii) schematic c-direction oriented crystal packing of PbI$_2$ crystal; and (iii) corresponding structure after intercalation with organic iodide (C12I).

Figure 3. TEM images of PbI$_2$ nanocrystals prepared in (a) acetonitrile and (b) methanol. (c) Corresponding electron diffraction pattern of (b).

nucleation and growth of PbI$_2$ single crystals. The final shape is attributed to minimizing surface energies [22], with the anisotropic growth mainly along the hexagonal plane rather than the c-axis ([0 0 1] direction), with corresponding anisotropic aspect ratios of ~5.9, 6.2 and 8.0 for PbI$_2$ crystals prepared in acetonitrile, methanol and ethanol, respectively.

Studies have previously been performed to observe the effect of intercalation time on IO hybrid crystal quality [21]. SEM images of the intercalated PbI$_2$ crystals (prepared in acetonitrile) reveal that longer durations (40 s) of intercalation of organic moiety (dissolved in toluene) indeed affect the surface morphology. However, complete intercalation takes less than 5 s [10] and sustained hexagonal shapes are preserved in crystals intercalated for 10 s (Fig. 2c)—hence the degradation can be avoided. During intercalation the parent PbI$_2$ layers exfoliate sequentially and between the Pb–I layers of C12PI, the Pb atoms are offset from layer to layer, which results in a staggered arrangement of $(PbI_6)^{4-}$ octahedra. Figure 2d(ii and iii) shows the schematic crystal structures of the parent PbI$_2$ and resultant C12PI phases. As a consequence of intercalation, the Pb–I network layers move much further apart from precise interlayer gaps of 6.78 Å to 24.91 Å [16] (Fig. 1). Therefore these hexagonal crystals exfoliate predominantly from about 400 nm to more than a micron thick along the c-axis and with minimal changes in the lateral directions of [1 1 0] and [1 0 0] (Fig. 2a(i)).
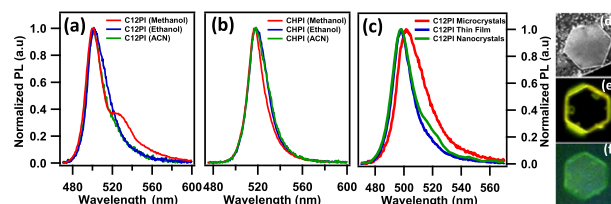
The crystals extracted via filtration show micron diameters, but the reactant solution in methanol also contains a range of crystal sizes down to a few tens of nanometers. These resultant solutions were transferred onto transmission electron microscopy (TEM) grids. The TEM images show that these PbI$_2$ crystals consist of dense nanometer-scale particles with diameters of 20–30 nm (Fig. 3a, b). The selected-area diffraction (SAD) patterns (Fig. 3c) indicate that the PbI$_2$ nano-

crystals are highly crystalline. The interplanar spacings (d-spacing) values from SAD patterns (6.988 and 3.470 Å) and from XRD (6.937 and 3.423 Å), for the [0 0 1] and [1 0 1] planes, respectively, are in close agreement. The strong diffraction from the [0 0 1] planes shows that the layered stacking arrangement in these nanocrystals is intact.

Essentially, these IO hybrids are naturally self-organized into "quantum-well" structures, in which a 2-D lead iodide semiconductor monolayer and an organic moiety monolayer are alternately stacked. As a result, such hybrids exhibit strong room-temperature excitons [12]. Figure 4 shows the room-temperature photoluminescence (PL) spectra of the IO hybrid crystals using a 404 nm laser excitation source. All C12PI (Fig. 4a) microcrystals show relatively narrow (full width at half maximum ~20 nm) and strong excitonic emissions at 497 nm. Similarly another IO hybrid, CHPI, prepared by the same method, also shows strong and narrow emission at 517 nm (Fig. 4b). The parent PbI$_2$ is a direct semiconductor with band gap of around 2.5 eV [23], and shows PL only at low temperatures, originating from exciton recombination and trapped electrons–hole pairs produced in band-to-band excitation [11] as well as a crystal-disorder-related broad emission band [15]. However, the strong room-temperature emission from these IO hybrids has been attributed to excitons formed within the inorganic layers by the transition from the lowest conduction band composed mainly of 6p Pb(II) atomic orbitals and the valence band containing an admixture of Pb^{2+} s and p and I$^-$ p states [24–26]. Figure 4a shows an additional red-shifted shoulder to that of main PL,

Figure 4. Room-temperature PL spectra of microcrystals of (a) C12PI (λ_{PL} = 498 nm) and (b) CHPI (λ_{PL} = 520 nm), prepared from various solvents. (c) Room-temperature PL of C12PI nanocrystals, microcrystals and thin film (obtained from conventionally synthesized C12PI). (d) Shows a SEM image of hexagonally shaped C12PI IO hybrid microcrystal (7 μm size). (e) and (f) show the corresponding dark-field microscopy image and photoluminescence ($_{ex}$ = 404 nm) image, respectively.

which is due to excitons from other high-temperature structural phase entities of C12PI [13].

Figure 4c compares the PL of C12PI nano/microcrystals to that of the PL obtained from thin films made out of conventionally synthesized C12PI. A clear red shift of 4 nm and broader PL emission is observed from the microcrystals, compared to the nanocrystal and thinfilm forms. This could possible due to strain build-up in the thick stack of layers in microcrystals (thickness > 700 nm) compared to the thin films (~80 nm) or nanocrystals (20–30 nm), which can result in structural rearrangements/distortions (such as distorted bond angles within $(PbI_6)^{4-}$ octahedra) [15,17].

The C12PI nanocrystals clearly preserve all the strong features of the hybrid thin-film optical properties. Here the excitons do not undergo surface recombination and/ or defect-related problems typical for inorganic/organic semiconductors patterned to nanometer sizes. Therefore, the exciton diffusion is low compared to that of typical microcrystals. In addition, the quantum confinement effects already seen from the strong vertical confinement in the inorganic/organic stacked sheets allow no further effects to be seen as the dimensions are reduced in the lateral directions.

Individual hexagonal microcrystals are also examined in a modified set-up consisting of a confocal microscope with facilities to image the PL from individual crystals by illumination with an excitation laser (404 nm) on the top face of a crystal [17]. Individual hexagonally shaped crystals (~7 μm) of C12PI have been selected (Fig. 4d). Figure 4e shows the dark-field confocal image using white light and Figure 4f is the PL image using a long-pass 410 nm filter. Such crystals exhibit a strong green-coloured emission which is confined to the periphery of the crystal edges, thus supporting the waveguiding effect. This study may thus lead to investigations of whispering gallery mode lasing in appropriately sizeselected individual crystals.

In conclusion, hexagonally shaped PbI_2 low-dimensional IO hybrid crystals (in the size range from 20 nm to several microns and with an average thickness (c-axis growth) of 400 ± 100 nm) were successfully synthesized via soft-chemistry-based techniques. The hexagonal shape of crystals and the minimized surface energies in the growth process arise from anisotropic growth preferentially along the hexagonal plane rather than the *c*-axis. The IO hybrids C12PI are then obtained by intercalating the organic iodide, C12I, into these PbI_2 crystals, by appropriately monitoring the growth dynamics, intercalation rate and surface morphology. These naturally self-organized IO hybrids, composed of alternating stacks of inorganic and organic semiconductors along the *c*-axis, show remarkable room-temperature PL due to quantum and dielectric confinement effects. C12PI microcrystals show red-shifted and broader PL than conventionally synthesized thin films, which is possibly due to structural distortions, such as distorted bond angles within $(PbI_6)^{4-}$ octahedra, due to strain build-up in the thick stack of layers in microcrystals (thickness > 700 nm). On the other hand, C12PI nanocrystals preserve all the strong optical features of thin films and do not suffer any surface recombination and/or defectrelated recombination, and therefore their exciton diffusion is low compared to that of microcrystals.

Supplementary data associated with this article can be found, in the online version, at http://dx.doi.org/ 10.1016/j.scriptamat.2012.07.048.

[1] D.B. Mitzi, K. Chondroulis, C.R. Kagan, IBM J. Res. Dev. 45 (2001) 29.
[2] G.C. Papavassiliou, I.B. Koutselas, Synth. Met. 71 (1995) 1713.
[3] R. Parashkov, A. Brehier, A. Georgiev, S. Bouchoule, X. Lafosse, J.S. Lauret, C.T. Nguyen, M. Leroux, E. Deleporte, in: N.H. Voler (Ed.), Prog. Adv. Mater. Res, Nova Science, 2007.
[4] S. Zhang, G. Lanty, J.S. Lauret, E. Deleporte, P. Audebert, L. Galmiche, Acta Mater. 57 (2009) 3301.
[5] G. Lanty, A. Brehier, R. Parashkov, J.S. Lauret, E. Deleporte, New J. Phys. 10 (2008) 065007.
[6] M. Baibarac, N. Preda, L. Mihut, I. Baltog, S. Lefrant, J.Y. Zevellec, J. Phys: Condens. Mat. 16 (2004) 2345.
[7] M.R. Tubbs Develop, Phys. Status Solidi B 49 (1972) 11.
[8] C.J. Sandroff, S.P. Kelty, D.M. Hwang, J. Chem. Phys. 85 (1986) 5337.
[9] K. Mallik, T.S. Dhami, Phys. Rev. B 58 (1998) 13055.
[10] K. Pradeesh, J.J. Baumberg, G. Vijaya Prakash, Appl. Phys. Lett. 95 (2009) 033309.
[11] C.C. Coleman, H. Goldwhite, W. Tikkanen, Chem. Mater. 10 (1998) 2794.
[12] M. Shimizu, J.I. Fujisawa, I.H. Junko, Phys. Rev. B 71 (2005) 205306.
[13] K. Pradeesh, J.J. Baumberg, G. Vijaya Prakash, Appl. Phys. Lett. 95 (2009) 173305.
[14] K. Pradeesh, J.J. Baumberg, G. Vijaya Prakash, J. Appl. Phys. 111 (2012) 013511.
[15] G. Vijaya Prakash, K. Pradeesh, R. Ratnani, K. Saraswat, M.E. Light, J.J. Baumberg, J. Phys. D 42 (2009) 185405.
[16] K. Pradeesh, G. Sharachandar Yadav, Monika Singh, G. Vijaya Prakash, Mater. Chem. Phys. 124 (2010) 44.
[17] K. Pradeesh, J.J. Baumberg, G. Vijaya Prakash, Opt. Express 17 (2009) 22171.
[18] K. Pradeesh, Monika Agarwal, K. Koteswara Rao, G. Vijaya Prakash, Solid State Sci. 12 (2010) 95.
[19] G. Zhu, P. Liu, M. Hojamberdiev, J.P. Zhou, X. Huang, B. Feng, R. Yang, Appl. Phys. A 98 (2010) 299.
[20] G.C. Papavassiliou, I.B. Koutselas, A. Terzis, M.H. Whangbo, Solid State Commun. 91 (1994) 695.
[21] Supplementary data.
[22] Z. Zheng, S.M. Wang, D.P. Li, A.R. Liu, B.J. Huang, H.X. Zhao, L.Z. Zhang, J. Cryst. Growth 308 (2007) 398.
[23] V. Mahrotra, S. Lambardo, M.O. Thompson, E.P. Giannelis, Phys. Rev. B. 44 (1991) 5786.
[24] Z. Xu, D.B. Mitzi, C.D. Dimitrakopoulos, K.R. Maxcy, Inorg. Chem. 42 (2003) 2031.
[25] I.C. Schluter, M. Schluter, Phys. Rev. B 9 (1974) 1652.
[26] J. Robertson, Solid State Commun. 26 (1978) 791.